15. Satin, J. *et al.* A mutant of TTX-resistant cardiac sodium channels with TTX-sensitive properties. *Science* **256,** 1202–1205 (1992).
16. Kaneko, Y., Matsumoto, G. & Hanyu, Y. TTX resistivity of Na+ channel in newt retinal neuron. *Biochem. Biophys. Res. Commun.* **240,** 651–656 (1997).
17. Yotsu-Yamashita, M. *et al.* Binding properties of 3H-PbTx-3 and 3H-saxitoxin to brain membranes and to skeletal muscle membranes of puffer fish *Fugu Pardalis* and the primary structure of a voltage-gated Na+ channel alpha-subunit (fMNa1) from skeletal muscle of *F. pardalis. Biochem. Biophys. Res. Commun.* **267,** 403–412 (2000).
18. Terlau, H. *et al.* Mapping the site of block by tetrodotoxin and saxitoxin of sodium channel II. *FEBS Lett.* **293,** 93–96 (1991).
19. Yamagishi, T., Li, R. A., Hsu, K., Marban, E. & Tomaselli, G. F. Molecular architecture of the voltage-dependent Na channel: functional evidence for alpha helices in the pore. *J. Gen. Phys.* **118,** 171–181 (2001).
20. Kallen, R. G. *et al.* Primary structure and expression of a sodium channel characteristic of denervated and immature rat skeletal muscle. *Neuron* **4,** 233–242 (1990).
21. Trimmer, J. S., Cooperman, S. S., Agnew, W. S. & Mandel, G. Regulation of muscle sodium channel transcripts during development and in response to denervation. *Dev. Biol.* **142,** 360–367 (1990).
22. Huey, R. B. & Moody, W. J. Neuroscience and evolution. Snake sodium channels resist TTX arrest. *Science* **297,** 1289–1290 (2002).
23. Zakon, H. H. Convergent evolution on the molecular level. *Brain Behav. Evol.* **59,** 250–261 (2002).
24. Lipkind, G. M. & Fozzard, H. A. KcsA crystal structure as framework for a molecular model of the Na+ channel pore. *Biochemistry* **39,** 8161–8170 (2000).
25. Plummer, N. W. & Meisler, M. H. Evolution and diversity of mammalian sodium channel genes. *Genomics* **57,** 323–331 (1999).
26. Raymond, C. K. *et al.* Expression of alternatively spliced sodium channel alpha-subunit genes: Unique splicing patterns are observed in dorsal root ganglia. *J. Biol. Chem.* **279,** 46234–46241 (2004).
27. Goldin, A. L. Resurgence of sodium channel research. *Annu. Rev. Physiol.* **63,** 871–894 (2001).
28. Choudhary, G., Yotsu-Yamashita, M., Shang, L., Yasumoto, T. & Dudley, S. C. Jr Interactions of the C-11 hydroxyl of tetrodotoxin with the sodium channel outer vestibule. *Biophys. J.* **84,** 287–294 (2003).
29. Penzotti, J. L., Fozzard, H. A., Lipkind, G. M. & Dudley, S. C. Jr Differences in saxitoxin and tetrodotoxin binding revealed by mutagenesis of the Na+ channel outer vestibule. *Biophys. J.* **75,** 2647–2657 (1998).
30. Stefani, E. & Bezanilla, F. Cut-open oocyte voltage-clamp technique. *Methods Enzymol.* **293,** 300–318 (1998).

....

Sodium channel mutation leading to saxitoxin resistance in clams increases risk of PSP

V. Monica Bricelj[1], **Laurie Connell**[2], **Keiichi Konoki**[3], **Scott P. MacQuarrie**[1], **Todd Scheuer**[3], **William A. Catterall**[3] & **Vera L. Trainer**[4]

[1]*Institute for Marine Biosciences, National Research Council, Halifax, Nova Scotia B3H 3Z1, Canada*
[2]*School of Marine Sciences, University of Maine, Orono, Maine 04469, USA*
[3]*Department of Pharmacology, University of Washington, Seattle, Washington 98195, USA*
[4]*NOAA Fisheries, Northwest Fisheries Science Center, Seattle, Washington 98112, USA*

....

Bivalve molluscs, the primary vectors of paralytic shellfish poisoning (PSP) in humans, show marked inter-species variation in their capacity to accumulate PSP toxins (PSTs)[1] which has a neural basis[2,3]. PSTs cause human fatalities by blocking sodium conductance in nerve fibres[4,5]. Here we identify a molecular basis for inter-population variation in PSP resistance within a species, consistent with genetic adaptation to PSTs. Softshell clams (*Mya arenaria*) from areas exposed to 'red tides' are more resistant to PSTs, as demonstrated by whole-nerve assays, and accumulate toxins at greater rates than sensitive clams from unexposed areas. PSTs lead to selective mortality of sensitive clams. Resistance is caused by natural mutation of a single amino acid residue, which causes a 1,000-fold decrease in affinity at the saxitoxin-binding site in the sodium channel pore of resistant, but not sensitive, clams. Thus PSTs might act as potent natural selection agents, leading to greater toxin resistance in clam populations and increased risk of PSP in humans. Furthermore, global expansion of PSP to previously unaffected coastal areas[6] might result in long-term changes to communities and ecosystems.

PSP, caused by human consumption of shellfish that feed on toxic algae, is a public health hazard and causes severe economic losses globally due to bans on harvesting of contaminated shellfish and the need for costly monitoring programmes. PSP-producing dino-flagellates (for example *Alexandrium* spp.) cause toxic blooms ('red tides') in North America and worldwide. PSTs block conduction of the nerve impulse by interfering with the voltage-dependent increase in sodium-ion conductance that generates the action potential in nerve and muscle fibres[4,5], leading to neuromuscular paralysis. Large differences in PST accumulation between bivalve species *in vivo*[1] have been associated with *in vitro* differences in sensitivity of isolated nerves to saxitoxin (STX), the most potent PST, and the related tetrodotoxin (TTX)[2,3]. STX and TTX bind to a single site in the outer pore of the Na+ channel, formed by the amino-acid residues in the outer-pore loops located between the S5 and S6 segments of each of the four homologous domains (I–IV) of the α-subunit[7,8]. Could differences in amino acid sequence in the receptor site for STX and TTX in Na+ channels cause differences
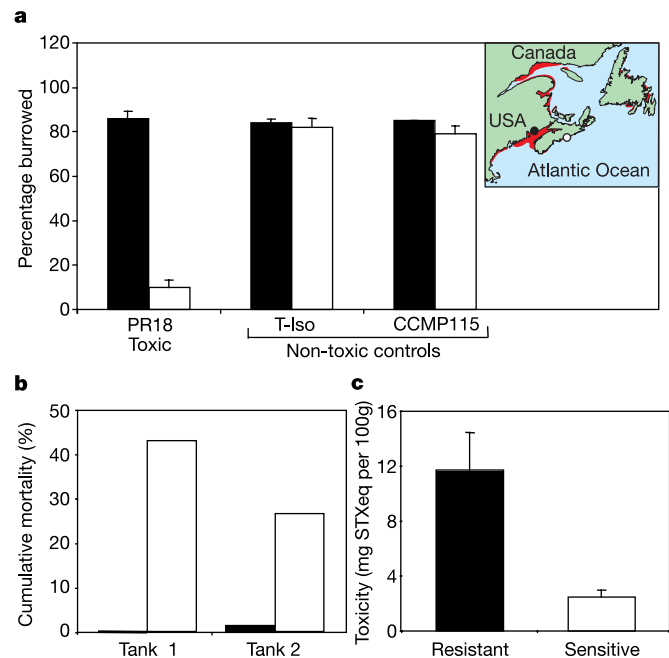

Figure 1 Responses to PSTs in two *M. arenaria* populations. **a**, Percentage of clams that burrowed after 24 h of exposure to *A. tamarense* (strains PR18b or CCMP115) or *I. galbana* (T-Iso) ($n = 2$ tanks). Map shows the study sites BF (filled circle) and LE (open circle); the PSP-affected coastline is in red. **b**, Mortality after 16 days of toxification with strain PR18b (determined by visual inspection (dead clams removed) (tank 1) and by removal of all clams every 2 days (live clams reintroduced in sediment) (tank 2)). In **a** and **b**, filled columns are results for BF clams, and open columns for LE clams. **c**, Tissue toxicity of live clams after 16 days of toxification of resistant BF and sensitive LE clams (burrowers and non-burrowers at 24-h, respectively). All results are means ± s.e.m.

in toxin sensitivity and accumulation in shellfish and thereby contribute to the risk of PSP? We have probed this question with a combination of behavioural, physiological and molecular biological approaches.

Mya arenaria is a commercially important native species with wide latitudinal distribution in Atlantic North America, from the Gulf of St Lawrence to Chesapeake Bay. We collected clams from two sites with contrasting histories of PSP (Fig. 1a inset): Lepreau Basin, Bay of Fundy (BF), where annual, recurrent toxic blooms of *Alexandrium* spp. occur in summer[9], and the Lawrencetown estuary (LE), Nova Scotia, an area with no record of PSP. Burrowing activity provided an index of susceptibility to toxins in clams[10]. After exposure to toxic *A. tamarense* cells for 24 h, most clams (a mean of 86%) from LE were unable to re-burrow after deployment at the sediment surface, whereas only 10% of clams from the BF population were compromised (Fig. 1a). Burrowing was not affected by exposure to non-toxic *Isochrysis galbana* (T-Iso) or to *A. tamarense* strain CCMP115, which is of negligible toxicity. Therefore burrowing incapacitation in susceptible clams is toxin-induced and is attributed to muscle paralysis. PSTs also prevented siphon retraction in susceptible clams[11]. Sublethal effects of PSTs on burrowing and siphon retraction in a high-energy, intertidal habitat, where clams can become exposed at the sediment surface, may cause indirect mortalities through desiccation and predation.

Longer-term laboratory exposure to toxic *A. tamarense* cells resulted in high differential mortalities between the two populations (Fig. 1b). Mortalities of LE clams were consistently higher (26–42% after 16 days of toxin exposure) than those of BF clams held under identical conditions (2% or less). LE clams also showed significantly lower feeding rates on toxic cells and decreased metabolic rates during toxification[11]. This individual variation in fitness-related traits provides a basis for natural selection.

To compare their toxin accumulation capacity, dominant phenotypes from the two populations were exposed to toxic *A. tamarense* for 16 days. Resistant BF clams (burrowers after 24 h of toxification) attained a mean toxicity significantly (fivefold) higher than sensitive LE clams (non-burrowers) (Fig. 1c, equal to a toxin concentration of 657 and 112 nmol g^{-1} respectively). Toxicities in both groups exceeded the regulatory safety level (80 µg STX equivalents per 100 g) and increased linearly at rates of 771 ($r^2 = 0.96$) and 113 µg STX equivalents per day ($r^2 = 0.80$) in resistant and sensitive clams, respectively (data not shown), resulting in more than an order of magnitude difference in toxicity among individuals after 2 weeks. *M. arenaria* field populations can attain toxicities (~9,600 µg STX equivalents per 100 g) comparable to those determined in this study and accumulate even higher toxin levels in the viscera[1].

In vitro exposure of isolated cerebrovisceral nerve trunks of naive (toxin-free) clams from BF and LE to serially increasing STX concentrations also revealed large (more than 100-fold) differences in sensitivity to STX between and within populations (Fig. 2a; compare results at 4 and 400 µM STX). Nerves from most clams in the LE population with no history of PSP (69%) experienced full block of the action potential at 33 µM STX within ~30 s (Fig. 2b, left). In contrast, most clams (91%) from the PSP-exposed population (BF) were resistant to 33 µM and even 334 µM STX, the highest concentration tested. These differences in response in naive clams indicate that they were not induced by toxins retained in tissues but were an intrinsic response of individual nerves to toxin exposure *in vitro*.

Site-directed mutations within the Na$^+$ channel pore region[12] and naturally occurring variations in amino acid sequences in the outer pores of different mammalian Na$^+$ channels[13,14] can result in a decreased binding affinity for STX and TTX and thus in an increased toxin resistance. To test the hypothesis that a mutation in the α-subunit Na$^+$ channel is responsible for the differences in STX sensitivity, we determined both the genomic and the complementary DNA sequence of the pore regions of Na$^+$ channels
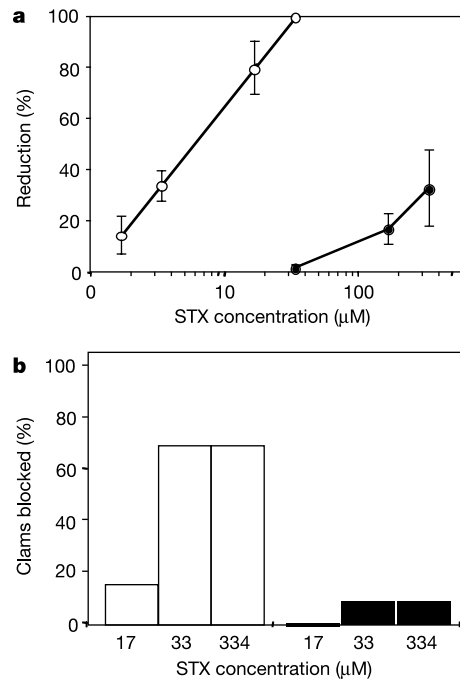

Figure 2 Nerve response of toxin-free, individual clams to STX *in vitro*. **a**, Percentage decrease in the compound action potential in isolated nerve preparations exposed to increasing STX concentrations relative to the pre-exposure condition. Values are amplitudes of the action potential of three representative sensitive (open circles) and three resistant (filled circles) clams (means ± s.e.m.). The response measured when the reduction was maximized (~5 min except for the 100% block, which occurs within seconds). **b**, Percentage of clams tested from each population exhibiting full action potential block in relation to STX concentration (the maximum tested was 334 µM; $n = 11$ BF clams (filled columns) and 13 LE clams (open columns)).

from sensitive and resistant *Mya arenaria* individuals, identified by using the nerve assay. Alignments of the predicted protein sequences encoded by the cDNAs showed striking similarities to known voltage-gated Na$^+$ channels from jellyfish to rat (Fig. 3). Alignments of all individual clam pore region sequences revealed a single-nucleotide mutation that correlated with clam resistance to STX. The genomic DNA and cDNA sequences were identical for each individual clam, showing that RNA editing[15] was not involved in generation of the mutated Na$^+$ channel protein. This mutation resulted in an amino-acid substitution in the outer pore loop of domain II from glutamic acid (E) to aspartic acid (D) at a position equivalent to E945 in rat Nav1.2a (ref. 16). Glutamic acid is found at this position in all wild-type (WT) Na$^+$-channel α subunits from a wide range of species (Fig. 3). Molecular models propose that this residue forms part of the outer pore lining and interacts with the hydroxyl groups at C-12 of STX[17]. Site-directed *in vitro* mutagenesis experiments have shown that it is a major determinant for STX binding[12]. Neutralization of this acidic residue by mutation to glutamine (Q) decreased STX affinity 19,880-fold and TTX affinity 290-fold compared with WT[18].

To assess the role of the E945D mutation in the block by STX *in vitro*, the mutation was introduced by means of a shuttle plasmid into the corresponding position of rat brain Nav1.2a channels. The mutant Na$^+$ channel produced currents with electrophysiological properties indistinguishable from those of the WT channel (Fig. 4a, b, and Supplementary Fig. S1). Application of 10 nM TTX blocked about half of the WT current, and 100 nM TTX blocked it almost completely (Fig. 4a, top). The half-maximal inhibitory concentration (IC_{50}) for WT was 11.2 ± 1.5 nM. In contrast, 1,000-fold more TTX (10 µM) blocked only ~20% of the current through E945D channels (Fig. 4a, bottom) and the IC_{50} increased about
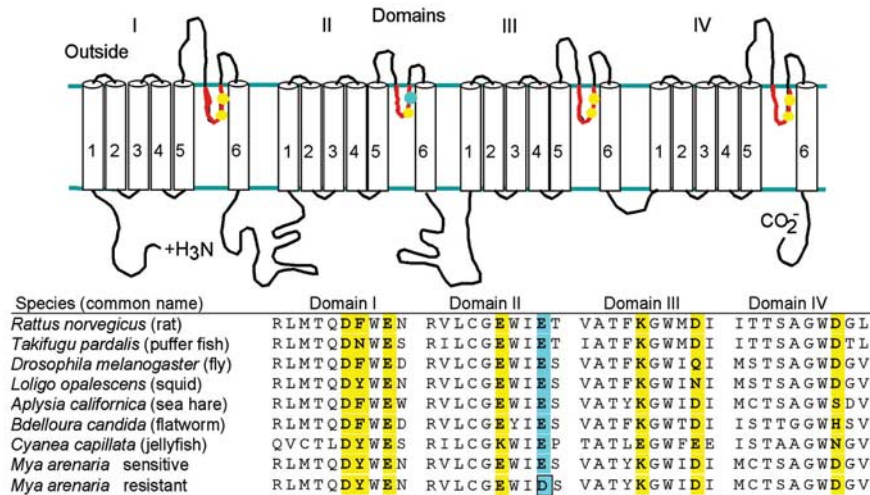
Figure 3 Mutation in the Na$^+$ channel pore of resistant *M. arenaria*. Top, primary structure of the Na$^+$ channel α-subunit, shown as a two-dimensional protein folding in and out of the cell membrane[8]. Cylinders represent transmembrane α-helices; solid lines represent hydrophilic portions of the sequence. Amino acids of the pore region (SS1 and SS2) in each domain are shown in red, and those associated with STX binding in yellow. Bottom, alignments of pore-forming loops (SS1, SS2) in each of four Na$^+$-channel domains in *M. arenaria* compared with those in other organisms, in descending phylogenetic order (GenBank database). Highlighted residues are crucial to STX binding[12,13]; position 945 (blue) in resistant *M. arenaria* is boxed.

3,000-fold to $35 \pm 9\,\mu M$ (Fig. 4c). Because STX is more potent, an order of magnitude less toxin was required to obtain a similar blocking effect. STX at 1 nM blocked 40% of WT current, and 10 nM STX blocked it nearly completely (Fig. 4b, top) (IC$_{50}$ = 1.7 ± 0.2 nM). In contrast, a 1,000-fold higher STX concentration (1 μM) blocked only 25% of the E945D current (Fig. 4b, bottom) (IC$_{50}$ ≈ 2.7 ± 0.6 μM; Fig. 4d). Thus, the E945D substitution made the Nav1.2a channel about 1,500-fold or 3,000-fold less sensitive to STX and TTX, respectively, and a similar decrease in affinity is expected in the *M. arenaria* Na$^+$ channel (see Supplementary Discussion). This is a surprisingly large reduction in binding affinity resulting from simply shortening of the side chain at position 945 by one methylene group without changing the negative charge of the carboxyl group. These results imply that this side chain is rigid in the outer vestibule of the channel and emphasize that even a small conformational change in the receptor site can result in a large decrease in the binding affinity of these toxins to Na$^+$ channels by altering the spatial relationships between ion-pair-forming and hydrogen-bond-forming partners.

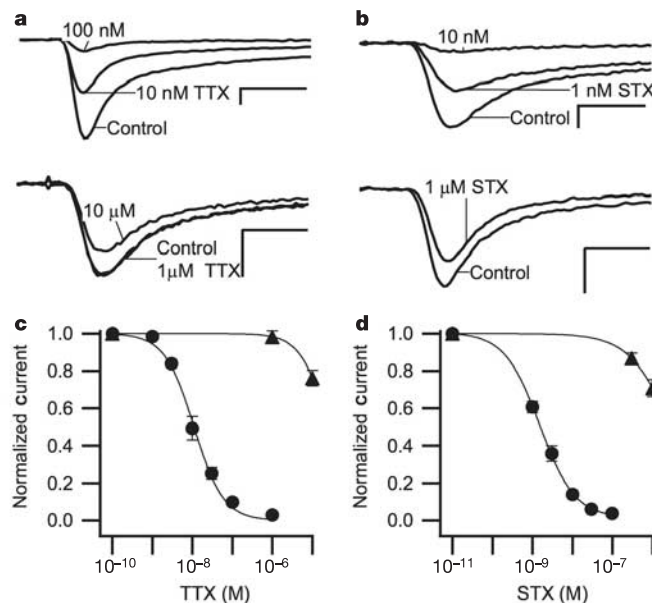Our results show that marked differences in whole-animal and

Figure 4 Blocking of WT and mutant Na$^+$ channels by TTX and STX. **a**, **b**, Na$^+$ currents in tsA-201 cells expressing WT (top) and E945D (bottom) channels and their blocking by TTX (**a**) and STX (**b**). Currents elicited by step depolarizations to −10 mV from a −120-mV holding potential. Scale bars, 1 nA and 1 ms. **c**, **d**, Inhibition curves for block of WT (circles) and E945D (triangles) by TTX (**c**) and STX (**d**). Peak Na$^+$ current normalized to its control is plotted against toxin concentration. Values are means ± s.d. for at least three determinations. Smooth curves were fitted with Langmuir isotherms to evaluate IC$_{50}$.

nerve susceptibility to PSTs and in toxin uptake capacity in *M. arenaria* result from a single mutation in domain II of the Na$^+$ channel pore region. These observed differences correspond to inter-population differences in the history of exposure to toxic blooms in the environment. The adaptive value of resistance to PSTs (increased survival) was also shown experimentally. Our results support the conclusion that *M. arenaria* populations in PSP-affected areas undergo genetic adaptation to toxins through selective mortality or reduced fitness of sensitive individuals. In this respect *M. arenaria* differ from Pacific butter clams, *Saxidomus giganteus*, in which PSTs function as an anti-predator defence[19].

A neural basis for inherited toxin resistance was shown in cattle ticks and house flies, in which a single Na$^+$ channel mutation confers resistance to pesticides (pyrethroids and DDT)[20,21]. Resistance to TTX in puffer fish *Takifugu (Fugu) pardalis*, which can accumulate high concentrations of TTX in tissue without adverse effects, has been attributed to a single mutation in the skeletal-muscle Na$^+$ channel[22], yet natural selection for resistance was not shown in this species. In terrestrial ecosystems, marked geographic variation in resistance to TTX in populations of garter snakes (*Thamnophis sirtalis*) has coevolved with that of its prey[23] (the toxic newt, *Taricha* sp.). Thus, different selective pressures (predation or toxic blooms) can lead to geographic differentiation in resistance to natural toxins within species. The increased accumulation of toxin in resistant *M. arenaria* points to this resistance mutation as an important risk factor for human PSP resulting from the consumption of this species. Our findings raise the possibility that other bivalve species might harbour similar mutations, thus allowing further understanding of the molecular basis of toxin resistance across shellfish species. □

Methods

Whole-animal observations

Juvenile clams (∼30–47 mm shell height), collected at a time of year when they contained no PSTs, were acclimated (16 °C, 30‰ salinity) for at least 2–3 weeks before experiments. Clams were toxified, as described previously[24], in aquaria containing coarse sand 10 cm deep, at a constant (100 cells ml^{-1}) bloom concentration of *A. tamarense* (isolate PR18b from the Gulf of St Lawrence; toxicity 60–98 pg STX equivalents per cell), maintained by cell delivery with a peristaltic pump[11]. Burrowing response was measured with previously described protocols[10] after exposure of clams to equal biovolume concentrations of either toxic or non-toxic cells.

For the measurement of survival, 40–50 clams from each population (BF and LE) were held together in each of two experimental tanks exposed to *A. tamarense* (PR18b). Mortalities were not averaged (Fig. 1b)—that is, tanks were not treated as replicates—because mortality determinations differed between the two systems (see the legend to Fig. 1b). Because of the lack of responsiveness of live but incapacitated (paralysed) clams, only clams exhibiting obvious signs of death (blackened and decomposing tissues, odour) were removed and included in mortality counts. Clams from both populations exposed in parallel to non-toxic *Thalassiosira weissflogii* suffered no mortalities over the course of the experiment.

To determine toxin accumulation, initially toxin-free clams were preselected (100 resistant BF clams and 120 sensitive LE clams based on the 24-h burrowing index) and then subjected to continued toxification in a common aquarium. The toxicity of algae and individual clams (five resistant BF and five sensitive LE clams) sampled every 2 days was determined by following methods described previously[11,24]. Individual PSTs were analysed by reverse-phase ion-pair high-performance liquid chromatography (HPLC) with fluorescence detection and converted to STX equivalents[25]. Toxin standards were obtained from the Institute of Marine Biosciences' Certified Reference Materials Program (CRMP). Final toxicities were compared by the analysis of variance and linear regressions fitted to toxicity data over time. The initial toxin-free status of experimental clams in all trials was confirmed by HPLC ($n = 3$–5).

Nerve electrophysiology was examined by the nerve test, adapted from Twarog[2,3], which was conducted at 14–15 °C using sections of nerve trunk no larger than 2 cm, without removal of the neural sheath. STX standard (3.48 mM in 0.1 M acetic acid) was diluted to required test concentrations (1.7–334 µM STX) in physiological saline solution (PSS) containing (in mM) 428 NaCl, 10 KCl, 20 MgCl$_2$.6H$_2$O, 10 CaCl$_2$.2H$_2$O and 50 Tris-HCl, adjusted to pH 7.4 with 1.0 M HCl and bubbled with air. Control tests indicated that the nerve response was not affected by acetic acid at the dilutions used (tested at constant pH) or by a pH of 5.6 or less. Thus no pH adjustment of the PSS was necessary for tests at 334 µM STX or less (the pH of the test solution was 6.2 to 7.4). Clams that showed a full action potential block at no more than 33 µM STX were characterized as sensitive, and those that required at least 334 µM STX to fully block were characterized as resistant.

Molecular genetics

For determination of the Na$^+$ channel sequence, nerve connectives dissected from living *M. arenaria* individuals were used for nerve assays, and the ganglia from the same individual were immediately transferred to RNAlater (Ambion) for storage. RNA was extracted from individual clam nerve tissue and stored in RNasecure (Ambion) at −80 °C.

First-strand cDNA was produced from isolated DNA-free RNA with the use of SuperScript II reverse transcriptase (Invitrogen) and random hexamer primers, followed by digestion with RNase H in accordance with the manufacturer's instructions. *M. arenaria*-specific Na$^+$-channel fragments were generated from the first-strand template by nested polymerase chain reaction (PCR) starting with domain IV and walking towards domain I. The complete cDNA sequence was determined for a fragment spanning domains I–IV (4,034 base pairs) using Big Dye Terminator Cycle Sequencing in an ABI 377 autosequencer (Applied Biosystems).

DNA and RNA were isolated from four individual clams from each site that had previously been subjected to nerve assays. Sequence from both the DNA and the resulting cDNA was obtained for each of the pore regions by using *M. arenaria*-specific PCR primers. The resulting PCR products were amplified and sequenced.

For the construction of Na$^+$ channel mutations, a two-step mutagenesis protocol, modified from previous methods[26], was followed to generate the specific E945D mutation through the shuttle vector pBluescript SK+/rNav 1.2a (*Xma*I > *Bst*EII) that contains the *Xma*I (nucleotide 1,896 in the loop between DI and II) to *Bst*EII (nucleotide 4,636 in domain IV region S1) into a fragment of full-length rat pCDM8/ Nav1.2a (rIIa) through the *Sph*I and *Bgl*II restriction sites.

Further details are given in Supplementary Methods.

Electrophysiology of transfected Na$^+$ channels

Human tsA-201 cells were transfected with cDNAs encoding WT or E945D mutant Nav1.2a channels by calcium phosphate precipitation, and Na$^+$ currents were recorded by whole-cell voltage clamp as described previously[27]. The extracellular solution contained (in mM) 140 NaCl, 5.4 CsCl, 1.8 CaCl$_2$, 1 MgCl$_2$, 10 Hepes (pH 7.35) at ∼23 °C. The intracellular saline contained (in mM) 189 *N*-methyl-D-glucamine (NMDG), 1 NaCl, 4 MgCl$_2$, 0.1 1,2-bis(2-aminophenoxy)ethane-*N*,*N*,*N'*,*N'*-tetraacetic acid (BAPTA), 25 Tris-phosphocreatine, 2 NaATP, 0.2 NaGTP and 40 Hepes, pH 7.35. TTX was obtained from Calbiochem, and STX standard (480 ± 20 µM STX in 0.1 M acetic acid) was from CRMP.

1. Bricelj, V. M. & Shumway, S. E. Paralytic shellfish toxins in bivalve mollusks: occurrence, transfer kinetics, and biotransformation. *Rev. Fish. Sci.* **6**, 315–383 (1998).
2. Twarog, B. M., Hidaka, T. & Yamaguchi, H. Resistance to tetrodotoxin and saxitoxin in nerves of bivalve mollusks. *Toxicon* **10**, 273–278 (1972).
3. Twarog, B. M. in *Proc. 2nd Int. Coral Reef Symp.* Vol. 1 (eds Cameron, A. M. *et al.*) 505–512 (Barrier Reef Committee, Brisbane, 1974).
4. Narahashi, T. & Moore, J. W. Neuroactive agents and nerve membrane conductances. *J. Gen. Physiol.* **51**, 93–101 (1968).
5. Hille, B. Pharmacological modifications of the sodium channels of frog nerve. *J. Gen. Physiol.* **51**, 199–219 (1968).
6. Hallegraeff, G. M. in *Manual on Harmful Marine Microalgae* (eds Hallegraeff, G. M., Anderson, D. M. & Cembella, A. D.) 25–49 (UNESCO, Paris, 2003).
7. Fozzard, H. A. & Hanck, D. Structure and function of voltage-dependent sodium channels: comparison of brain II and cardiac isoforms. *Physiol. Rev.* **76**, 887–926 (1996).
8. Catterall, W. A. From ionic currents to molecular mechanisms: the structure and function of voltage-gated sodium channels. *Neuron* **26**, 13–25 (2000).
9. Martin, J. L. & Richard, D. in *Harmful and Toxic Algal Blooms* (eds Yasumoto, T., Oshima, Y. & Fukuyo, Y.) 3–6 (International Oceanographic Commission of UNESCO, Paris, 1996).
10. Bricelj, V. M., Cembella, A. D., Laby, D., Shumway, S. E. & Cucci, T. L. in *Harmful and Toxic Algal Blooms* (eds Yasumoto, T., Oshima, Y. & Fukuyo, Y.) 405–408 (International Oceanographic Commission of UNESCO, Paris, 1996).
11. MacQuarrie, S. P. *Inter- and Intra-population Variability in Behavioral and Physiological Responses of the Softshell Clam,* Mya arenaria, *to the PSP Toxin-producing Dinoflagellate,* Alexandrium tamarense. Thesis, Dalhousie Univ. (2002).
12. Terlau, S. H. *et al.* Mapping the site of block by tetrodotoxin and saxitoxin of sodium channel II. *FEBS Lett.* **293**, 93–96 (1991).
13. Satin, J. *et al.* A mutant of TTX-resistant cardiac sodium channels with TTX-sensitive properties. *Science* **256**, 1202–1205 (1992).
14. Sivilotti, L., Okuse, K., Akopian, A. N., Moss, S. & Wood, J. N. A single serine residue confers tetrodotoxin insensitivity on the rat sensory-neuron-specific sodium channel SNS. *FEBS Lett.* **409**, 49–52 (1997).
15. Jaenisch, R. & Bird, A. Epigenetic regulation of gene expression: how the genome integrates intrinsic and environmental signals. *Nature Genet.* **33** (Suppl.), 245–254 (2003).
16. Auld, V. J. *et al.* A neutral amino acid change in segment IIS4 dramatically alters the gating properties of the voltage-dependent sodium channel. *Proc. Natl Acad. Sci. USA* **87**, 323–327 (1990).
17. Lipkind, G. & Fozzard, H. A. A structural model of the tetrodotoxin and saxitoxin binding site of the Na$^+$ channel. *Biophys. J.* **66**, 1–13 (1994).
18. Kontis, K. J. & Goldin, A. L. Site-directed mutagenesis of the putative pore region of the rat IIA sodium channel. *Mol. Pharmacol.* **43**, 635–644 (1993).
19. Kvitek, R. G. & Beitler, M. K. Relative insensitivity of butter clam neurons to saxitoxin: a pre-adaptation for sequestering paralytic shellfish poisoning toxins as a chemical defense. *Mar. Ecol. Prog. Ser.* **69**, 47–54 (1991).
20. Liu, M.-Y., Bull, D. L. & Plapp, F. W. Jr Effects of exposure to cypermethrin on saxitoxin binding in susceptible and pyrethroid-resistant houseflies. *Arch. Insect Biochem. Physiol.* **37**, 73–79 (1998).
21. He, H. *et al.* Identification of a point mutation in the para-type sodium channel gene from a pyrethroid-resistant cattle tick. *Biochem. Biophys. Res. Commun.* **261**, 558–561 (1999).
22. Yamashita, M.-Y. *et al.* Binding properties of ^{3}H-PbTx-3 and ^{3}H-saxitoxin to brain membranes and to

skeletal muscle membranes of puffer fish *Fugu pardalis* and the primary structure of a voltage-gated Na$^+$ channel α-subunit (fMNa1) from skeletal muscle of *F. pardalis*. *Biochem. Biophys. Res. Commun.* **267**, 403–412 (2000).

23. Geffeney, S., Brodie, E. D. Jr, Ruben, P. C. & Brodie, E. D. III Mechanisms of adaptation in a predator-prey arms race: TTX-resistant sodium channels. *Science* **297**, 1336–1339 (2002).

24. Bricelj, V. M., Lee, J. H. & Cembella, A. D. Influence of dinoflagellate cell toxicity on uptake and loss of paralytic shellfish toxins in the northern quahog, *Mercenaria mercenaria* (L.). *Mar. Ecol. Prog. Ser.* **74**, 33–46 (1991).

25. Oshima, Y. in *Manual on Harmful Marine Microalgae* (eds Hallegraeff, G. M., Anderson, D. M. & Cembella, A. D.) 81–94 (International Oceanographic Commission Manuals and Guides 33, UNESCO, Paris, 1995).

26. Storici, L., Lewis, K. & Resnick, M. A. In-vivo site-directed mutagenesis using oligonucleotides. *Nature Biotechnol.* **19**, 773–776 (2001).

27. Linford, N. J., Cantrell, A. R., Qu, Y., Scheuer, T. & Catterall, W. A. Interaction of batrachotoxin with the local anesthetic receptor site in transmembrane segment IVS6 of the voltage-gated sodium channel. *Proc. Natl Acad. Sci. USA* **95**, 13947–13952 (1998).

....

Ipr1 gene mediates innate immunity to tuberculosis

Hui Pan[1]*, Bo-Shiun Yan[1]*, Mauricio Rojas[1,3]*, Yuriy V. Shebzukhov[1]†, Hongwei Zhou[2], Lester Kobzik[2], Darren E. Higgins[4], Mark J. Daly[5], Barry R. Bloom[1] & Igor Kramnik[1]

[1]*Department of Immunology and Infectious Diseases and*
[2]*Physiology Program, Department of Environmental Health, Harvard School of Public Health, 667 Huntington Avenue, Boston, Massachusetts 02115, USA*
[3]*Grupo de Inmunología Celular e Inmunogenética, Facultad de Medicina, Universidad de Antioquia, Medellín, Colombia*
[4]*Department of Microbiology and Molecular Genetics, Harvard Medical School, Boston, Massachusetts 02115, USA*
[5]*Whitehead Institute for Biomedical Research, Cambridge, Massachusetts 02142, USA*

* These authors contributed equally to this work
† Present address: Department of Molecular Immunology, A. N. Belozersky Institute of Physical and Chemical Biology, Moscow State University, Vorobjovy Gory, Moscow, 119899, Russia

....

An estimated eight million people are infected each year with the pathogen *Mycobacterium tuberculosis*, and more than two million die annually[1]. Yet only about 10% of those infected develop tuberculosis. Genetic variation within host populations is known to be significant in humans and animals[2,3], but the nature of genetic control of host resistance to tuberculosis remains poorly understood. Previously we mapped a new genetic locus on mouse chromosome 1, designated *sst1* (for super-susceptibility to tuberculosis 1)[4]. Here we show that this locus mediates innate immunity in *sst1* congenic mouse strains and identify a candidate gene, *Intracellular pathogen resistance 1* (*Ipr1*), within the *sst1* locus. The *Ipr1* gene is upregulated in the *sst1* resistant macrophages after activation and infection, but it is not expressed in the *sst1* susceptible macrophages. Expression of the *Ipr1* transgene in the *sst1* susceptible macro-phages limits the multiplication not only of *M. tuberculosis* but also of *Listeria monocytogenes* and switches a cell death pathway of the infected macrophages from necrosis to apoptosis. Our data indicate that the *Ipr1* gene product might have a previously undocumented function in integrating signals generated by intracellular pathogens with mechanisms controlling innate immunity, cell death and pathogenesis.

It is estimated that about one-third of the human population on the planet has been infected by virulent *M. tuberculosis*[1,5]. Susceptibility to clinical tuberculosis is known to be influenced by environmental factors such as stress, malnutrition, concomitant infections (for example HIV) or senescence[6,7]. Although genetic variation within host populations is also known to affect resistance and susceptibility, individual genes responsible for innate immunity to the pathogen have been elusive. In susceptible individuals, progression of lung tuberculosis often leads to the formation of characteristic necrotic 'cavities' that destroy significant portions of the lung. Beyond their life-threatening clinical consequences, these lesions are essential for the efficient transmission of *M. tuberculosis* in aerosols. Because tuberculosis in humans is transmitted primarily by the respiratory route, the ability to cause lung disease is considered a key aspect of the pathogen's virulence strategy and ensures its evolutionary success. Therefore, understanding pathogenic mechanisms that are employed by virulent *M. tuberculosis* during lung tuberculosis in susceptible individuals is essential for developing effective prevention and treatment strategies[8,9]. However, detailed mechanistic studies of pathogenesis of lung tuberculosis and its genetic control have been limited by the fact that in mouse models of *M. tuberculosis* infection, necrotic lesions in the lungs are rarely found unless the mouse is rendered systemically immunodeficient.

C3HeB/FeJ inbred mice are extremely susceptible to virulent *M. tuberculosis* and develop a marked lung pathology, which leads to their rapid death after infection[10,11]. We generated a congenic mouse strain C3H.B6-*sst1* (*sst1*^{R}) carrying the C57BL/6J-derived resistant allele at the *sst1* locus on the C3HeB/FeJ genetic background. The survival time of the *sst1*^{R} congenic mice infected either with a high dose of intravenous *M. tuberculosis* (Fig. 1a) or with a low dose of *M. tuberculosis* by the respiratory route (Fig. 1b), relative to their *sst1*^{S} counterparts, is significantly lengthened, indicating a profound effect of the locus on anti-tuberculosis immunity. However, the shorter survival of the C3H.B6-*sst1* (*sst1*^{R}) mice, in comparison with the resistant parental strain C57BL/6J (B6), indicates that the *sst1* locus is responsible for a significant portion, but not all, of the tuberculosis resistance phenotype of the B6 mice.

The specific effect of the *sst1* locus on the progression of tuberculosis was related to a more efficient control of *M. tuberculosis* multiplication, primarily in the lungs, after both respiratory challenge by aerosol (Fig. 1c) and systemic intravenous infection (Supplementary Fig. 2a). The development of large necrotic lung lesions within 4 weeks after intravenous infection, characteristic of *sst1*^{S} mice, was prevented in the presence of the *sst1*^{R} allele (Fig. 1d). After a low-dose aerosol infection, chronic tuberculosis infection ensued, and the *sst1*^{S} mice developed encapsulated necrotic lung lesions, in some cases reaching about one-third of the lung lobe (Fig. 1e), that resembled tuberculosis cavities in human lungs. Mycobacteria were present both extracellularly, within necrotic central areas surrounded by the fibrotic capsule, and within macrophages of the granuloma wall (Supplementary Fig. 1). In the *sst1*^{R} mice, lung lesions were much smaller and contained fewer infected macrophages.

Although the greatest effect of the *sst1* polymorphism on the progression of tuberculosis was observed in the lungs, bone marrow transplantation experiments showed that bone marrow-derived cells, but not lung cells, were responsible for the effect of the *sst1* locus (Supplementary Fig. 2b). It is known that T lymphocytes and macrophages are of major importance in host resistance to tuberculosis. We have found that, whereas T lymphocytes are functionally